Biointerface Research in Applied Chemistry

Review Article

Open Access Journal

Utilization of carbon nanotube and graphene in electrochemical CO_2 reduction

Xueliang Sun [1], Qi Zhang [1], Qingqing Li [1], Zhang Xurui [1], Xiaolin Shao [1], Jin Yi [1], Jiujun Zhang [1], Yuyu Liu [1,*]

[1]Institute for Sustainable Energy/Collage of Science, Shanghai University, 99 Shangda Road, Shanghai 200444, China

corresponding author e-mail address: liuyuyu@shu.edu.cn, liuyuyu2014@126.com | Scopus ID 42261826700

ABSTRACT

The electrochemical reduction of carbon dioxide ($ERCO_2$) driven by renewable energy to produce low-carbon fuels and value-added chemicals has been well known as a way capable of simultaneously solving energy exhaustion and global warming issue. Catalysts play a vital role in low temperature $ERCO_2$, and those well used are single metals, metal oxides and alloys. Due to the characteristics of nanometer size, low resistance, high surface area, chemical stability, special mechanical and electronic properties, some novel carbon nomaterials (e.g. carbon nanotubes (CNTs) and graphene) show excellent properties in $ERCO_2$ as catalysts or supports which can improve the electrochemical performance: activity, selectivity, and stability. Actually, they mostly act as support materials and little directly as catalysts. The specific surface area and the active sites of loaded catalysts can be increased, then the performance is significantly improved. In this work, we will make a review on the progress as to CNTs and graphene as catalysts and supports in $ERCO_2$ in recent years and give the future prospects.

Keywords: *CO_2; electrochemical reduction; carbon nanotube; graphene; catalyst; support.*

1. INTRODUCTION

The gas emission caused by fossil fuel combustion has resulted in a remarkable carbon dioxide (CO_2) accumulation in atmosphere (as shown in Figure 1), followed by global warming. Meanwhile, fossil fuel reserves also fall rapidly. Therefore, it is vital to look for clean and sustainable energy such as solar, wind and tide energy. Conversion of CO_2 to valuable chemicals and low-carbon fuels is considered to be a promising way, because it may promote not only waste (gas) utilization but also energy storage. Among many available approaches (e.g. chemical, photocatalytic and electrocatalytic methods) to recycle the CO_2, the electrochemical reduction of CO_2 ($ERCO_2$) has a considerable potential economy and technical feasibility since it can convert those renewable energies and idle nuclear/water electrical energy into useful products.

As to the $ERCO_2$, there are basically three types of technologies which are applied at low temperature and high temperature [1-5]. In this work, we only focus on the low temperature process, which has obvious advantages over high temperature ones. However, low temperature $ERCO_2$ does require efficient and robust catalysts to lower the reaction overpotential and to minimize energy consumption. The lack of cost-effective catalysts with high activity, selectivity and stability is one of the biggest obstacles for realizing efficient $ERCO_2$ [2,3].

The carbon-based nanomaterials such as carbon nanotubes (CNTs) and graphene have been well used for energy storage and conversion as support material due to their nanometer size, low electric resistance, high surface area and chemical stability, and

special mechanical and electronic properties [6]. After being loaded, the specific surface area and active sites of catalysts can be increased and the electrochemical performance is popularly improved [7-17]. Besides, both of them may also directly act as the catalysts of $ERCO_2$ [18-21]. Compared to other carbon materials like carbon fibers [22], boron-doped diamond [23-25], nanoporous carbon [26] and even graphene dots [27-29], which are also used for the catalysis of $ERCO_2$, CNTs [30-34] and graphene [35-39] have attracted more attention recently, both of which, therefore, will be discussed here.
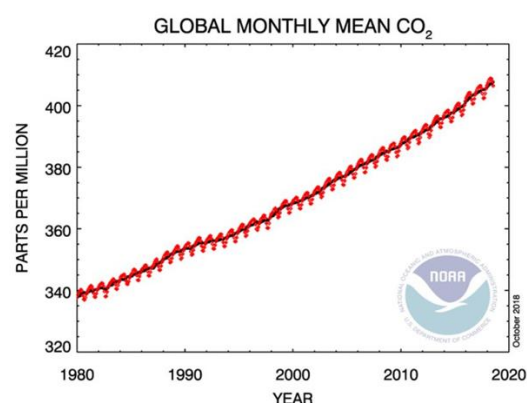

Figure 1. Full record global CO_2 (the dashed red line with diamond symbols represents the monthly mean values, centered in the middle of each month. The black line with the square symbols represents the same, after correction for the average seasonal cycle) (Photo courtesy of Brian Vasel, NOAA, Boulder, Colorado, USA (https://esrl.noaa.gov/gmd/))

2. CARBON NANOTUBES AS CATALYST SUPPORTING MATERIALS IN ERCO$_2$

CNTs are an allotrope of carbon with a cylindrical nanostructure and classified as single-walled carbon nanotube (SWCNT) and multi-walled carbon nanotube (MWCNT). As described above, CNTs can act as catalyst support owing to their

extraordinary thermal conductivity, mechanical and electrical properties, and high surface area [6]. Moreover, the resistance to acid/basic media, the capability of controlling the porosity and surface chemistry within certain limits, nanometer size, low

resistance, chemical stability, special mechanical, and electronic properties are also the important reasons [40]. As using CNTs as catalyst support to reduce CO_2, nanoscale metal catalysts are dispersed on CNTs [40]. CNTs have been combined with not only precious metals forming Pd-CNTs [41], Ag-CNTs, Ir-CNTs, Pt-CNTs [42], and Au-CNTs but also non-precious ones to Mn-CNTs [43], Fe-CNTs, Co-CNTs, Ni-CNTs [44], Cu-CNTs [32,45] and Sn-CNTs [46].

Mn is an abundant and inexpensive mental element and its metal complexes are found to be effective in the application to reduce CO_2. For example, [Mn(bpy)(CO)$_3$X] (bpy=2,2'-bipyridine; X=Cl$^-$, Br$^-$ or solvent) is known as highly effective precursors to catalysts for the $ERCO_2$ to CO, compared with those expensive [Re^1(bpy)(CO)$_3$X] [47]. As a non-precious metal material, [Mn(bpy)(CO)$_3$X] does not require relatively high overpotential for CO_2 reduction, but needs addition of a proton source for any activity to be observed [43,48-50]. Although adding protic solvent is benefit to the $ERCO_2$, the solubility issues actually prevent [Mn(bpy)(CO)$_3$X] from being used for CO_2 reduction in aqueous solution. To improve the catalytic performance, Walsh *et al* [43] developed a simple membrane supported manganese catalyst (e.g. Nafion/MWCNT/[Mn(bpy)(CO)$_3$Br]). The results showed that addition of MWCNTs led to a ~10 fold current enhancement (3 mA/cm^2 vs. 0.3 mA/cm^2) at −1.4 V$_{Ag/AgCl}$ at pH7. Recently, Sato *et al* [51] prepared a new Mn complex electrocatalyst, [Mn(4,4'-di(1H-pyrrolyl-3-propyl carbonate)-2,2'-bipyridine)(CO)$_3$MeCN]$^+$(PF$_6$)$^-$ ([Mn-MeCN]) loaded on conductive MWCNTs ([Mn-MeCN]/MWCNT). Compared with the bare [Mn-MeCN] cathode which was unhelpful to CO_2 reduction reaction in an aqueous solution, the [Mn-MeCN]/MWCNT electrode could efficiently promote the $ERCO_2$ to CO. The results showed that Mn-complex/MWCNT electrode could produce CO at a constant rate for 48 h and had a high current density than 2.0 mA/cm^2 at −0.39 V$_{RHE}$. Meanwhile the as-prepared electrode had a very low overpotential (ca. 100 mV) than previous reported Mn-complex catalysts.
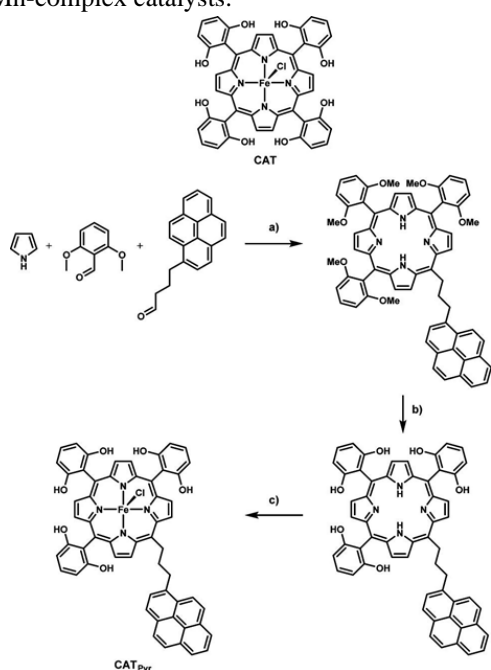

Figure 2. Covalent immobilization of the iron porphyrin catalyst CAT$_{pyr}$ on MWCNTs [56].
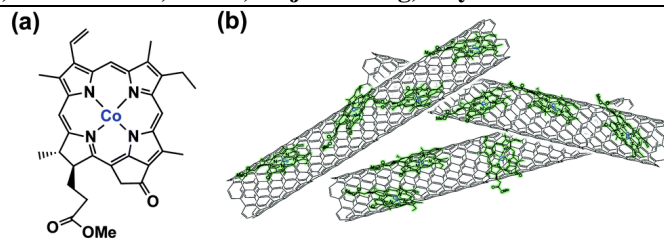

Figure 3. (a) Structure of CoII(Ch) and (b) schematic image of CoII(Ch) on MWCNTs [59].

Fe, which is a more inexpensive metal material compared with Mn, has also been used to prepare the catalysts for $ERCO_2$. Hori *et al* [52] had an early used Fe electrode to reduce CO_2 in aqueous KHCO$_3$ solution at −0.91 V$_{SHE}$. H$_2$ was measured to be the major product (FE$_{H_2}$=94.8%). After Fe being deposited on CNTs (the CNTs was annealed at 700°C in inert gas, and then treated in HNO$_3$ to introduce oxygen functionalities on the carbon surface) as the catalyst, it was found that FE$_{H_2}$ decreased to 80.6% and FE$_{CO}$ increased to 18.9% [53]. Zhao *et al* [54] prepared the electrodes modified with Fe porphyrin and CNTs (FeP-CNTs) for $ERCO_2$. Compared with the electrodes modified only with Fe porphyrin or CNTs, the FeP-CNTs electrode exhibited less negative cathode potential and higher reaction rate. The order of electrocatalysis efficiency was measured to be: FeP-CNTs > FeP > CNT. This high efficiency electrocatalysis of FeP-CNTs mainly came from two factors. First, the interaction between MWCNTs and Fe porphyrin reduced the overpotential to reduce CO_2 to formic acid. Second, the excellent conductivity of MWCNTs promoted electron transfer between CO_2 and the active site. Maurin *et al* [55] prepared FeP-CNTs by using a different method: covalent grafting Fe porphyrin on CNTs. The FeP-CNTs had high selectivity and activity for the $ERCO_2$ in water (pH=7.3) at low overpotential (0.5V). After 1h, the catalytic selectivity was 90% toward CO, and then it slightly decreased to 80% after 3h. Later, they used an improved Fe porphyrin catalyst (pyrene-appended iron triphenyl porphyrin bearing six pendant OH groups on the phenyl rings in all ortho and ortho' positions, namely CAT$_{pyr}$) to prepare the CAT$_{pyr}$/MWCNTs catalyst. Figure 2 shows that CAT$_{pyr}$ was immobilized on CNTs by noncovalent interactions. This new catalyst deposited onto a glassy carbon electrode reduced CO_2 to CO at low overpotential (480mV) in water (pH=7.3) and sustained for hours without loss of activity and selectivity [56]. Iron and nitrogen-doped carbon materials have recently been found to be cheap, stable and active alternatives. Jia *et al* [57] prepared the Fe/Fe$_3$C@NCNT catalyst (Fe/Fe$_3$C nanoparticles embedded in nitrogen-doped CNTs), the highest FE$_{CO}$ was 50% at −0.74 V$_{RHE}$ in 0.5M NaHCO$_3$. The good performance of the Fe/Fe$_3$C@NCNT catalyst was due to a large specific surface area and high content existence of N with pyridinic-N and pyrrolic-N bonding.
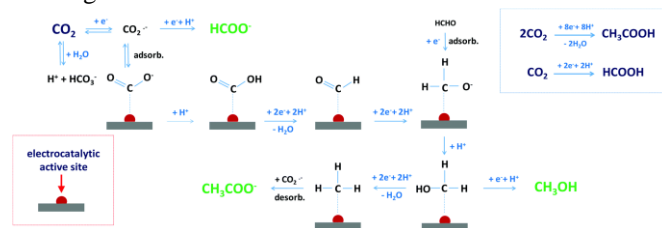

Figure 4. Schematic mechanistic pathway for the electrocatalytic production of formic acid, acetic acid and methanol on Cu10-CNT/GDL [64].
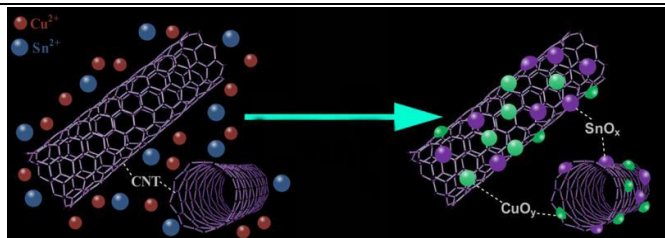
Figure 5. The structure of the Cu/SnOx-CNT catalyst [65].

Co and Fe are in the same Group(VIII). Like Fe, pure Co was also investigated in $ERCO_2$ in aqueous solution. However, the study showed that Co macrocycles had high catalytic selectivity for the production of H_2 [58]. To enhance its selectivity of non-hydrogen products, Shoko *et al* prepared the $Co^{II}(Ch)$ catalysts by adsorbing Co chlorin complex ($Co^{II}(Ch)$) on MWCNTs (Figure 3). The results indicated that the $Co^{II}(Ch)$ catalysts could reduce CO_2 to CO in H_2O (pH=4.6) with a high FE_{CO} (89%) at -1.1 V_{NHE}, which may be attributed to the three dimensional assembly of MWCNTs with Co^{II} (Ch) on the electrode surface and the π-π interaction between MWCNTs and Co^{II} (Ch) providing a suitable hydrophobic environment for binding of CO_2 [59].

As one of the non-precious metals, pure Cu is also a promising catalyst for the $ERCO_2$. However, the previous works show that Cu has low product selectivity [60]. For example, using Cu electrode as catalyst in 0.1 M $KHCO_3$ aqueous solution ($18.5\pm0.5°C$) at $-1.44V_{SHE}$ gave various products, and FE_{H_2} was high up to 20.5% [52,53]. Later, Baturina *et al* [61] supported Cu NPs on SWCNTs to prepare the Cu-SWCNTs catalyst. Compared with electrodeposited Cu electrode (Cu electrodeposition on Pt disk electrodes), the Cu-SWCNTs were more selective toward C_2H_4 generation, and had a significant (ca. 200 mV) shift in onset potentials, probably because of the increasing number of low-coordination sites (e.g. corners, edges, and defects) on the electrode surface. Hossain *et al* [45] used a series of CNT-supported Nano Cu (3-60nm) to catalyze the $ERCO_2$. The catalysts were prepared by homogeneous deposition precipitation method with urea as precipitating agent. When 20 wt. % copper was loaded on CNTs, the catalysts showed the maximum activity owing to the best balance of the amount of metal active sites and metal particle size. The CO_2 reduction had a high current density at the range of $0\sim-3$ V_{SHE}, and FE_{CH_3OH} was 38.5%.

Koo *et al* [62] electrochemically deposited Cu on aligned CNT sheets to prepare the oxygen-plasma-treated Cu-CNTs (O-CNT/Cu) electrocatalysts. The products were CO and methane, and the yields were 178 μmol cm²/mA·h and 346 μmol cm²/mA·h, respectively, and higher than CNT/Cu and CNT sheets. Marepally *et al* [63] used the Cu nanowires (NWs) as the catalyst precursor for the deposition Cu NPs onto CNTs to prepare the Cu NPs/CNTs catalyst by different methods, e.g. (1) the conventional impregnation route (ImR) to prepare the CuCNT-ImR catalyst; (2) use of Cu NWs as a copper precursor to prepare the CuCNT-NW catalyst. The main products were formic acid and CH_3COOH. Compared with the o-CNT (preliminarily activated with HNO_3 to create oxygen functional groups on their external surface) and CuCNT-ImR, the production rate toward the formic acid of the CuCNT-NW catalyst was 3 times higher than them. Later, Genovese *et al* [64] also deposited CNTs and Cu NPs on a gas diffusion layer (GDL) to prepare the Cu-CNT/GDL catalyst, and studied the mechanism. The Cu-CNT/GDL electrode could reduce CO_2 to CH_3COOH with a

high FE_{CH_3COOH} (56%) at room temperature and atmospheric pressure, and the only other products of reaction detected were formic acid and methanol (the latter in some cases), besides H_2. The mechanistic was described in Figure 4. After that, the researchers began to deposited Cu metal with other metals on CNT. Genovese *et al* [53] found that the FeCu-CNTs electrode could double the productivity to C1-C3 hydrocarbons/organics with respect to Fe monometallic electrocatalysts. Also, the deposition of Cu metal with other metal oxides loaded on CNT was researched. Huo *et al* [65] supported Cu and SnOx on the CNTs to prepare the Cu/SnOx-CNT catalyst (Figure 5). When the ratio of Cu and SnOx was different, and the $ERCO_2$ products formed were also different. That was when the catalyst contained 6.2% SnOx, CO_2 could be reduced with a high FE_{CO} (89%) and the current density was 11.3 mA/cm² at -0.99 V_{RHE}; when it contained 30.2% SnOx, CO_2 could be reduced with a high FE_{HCOOH} (77%) and the current density was 4.0 mA/cm² at -0.99 V_{RHE}.

Sn is one another of the widely-studied catalysts for the $ERCO_2$. In the early works, the Sn bulk was used to reduce CO_2 to produce formate. With the development of electrocatalysts, the researchers introduce the concept of the porous electrocatalysts on high surface area conductive support to make the performance of catalyst better. Chen *et al* [66] reported a 3D hierarchical porous structured CNT aerogel-supported Sn spheroidal particles (Sn/CNT-Agls) on carbon cloth (Sn/CNT-Agls/CC) electrode. The Sn/CNT-Agls electrochemically reduced the CO_2 to formate with high selectivity. The highest $FE_{formate}$ was 82.7% at a low overpotential of 361 mV, and the current density was 32.9 mA/cm². Compared with the Sn/CNT catalyst (CNT-supported Sn spheroidal particles), the Sn/CNT-Agls catalytic performance was greatly enhanced. The reason was that Sn/CNT-Agls catalyst had a high specific surface area, superior conductivity and excellent 3D hierarchical structure. Figure 6 exhibits typical SEM images of Sn/CNT-Agls (a and b). Sn metal oxides supported on CNTs are also investigated as catalyst for electrochemical CO_2 reduction. Bashir *et al* [46] reported the SnO_2/MWCNT electrocatalysts for CO_2 reduction in an aqueous electrolyte solution. It was found that when the content of SnO_2 was 20%, the catalysts showed the best performance, and could reduce CO_2 with a high $FE_{formate}$ (27.2%) as well as a high current density of 80 mA/cm² at -1.7 V_{SCE}. The good performance was attributed to high electrical conductivity and high surface area of the MWCNT, which contributed to obtain more active sites and disperse evenly at the electrode surface.

Re and its complexes have received wide attention due to its good catalytic properties. Rezaei *et al* [67] prepared the $[ReCl(CO)_3(\mu\text{-}tptzH)Re(CO)_3]$ electrocatalyst (where tptz-H = 2,4,6-tri(pyridine-2-yl)-2H-1,3,5-triazine-1-ide) for homogeneous and heterogeneous reduction of CO_2 in solution and on a carboxylated MWCNT modified pencil graphite electrode (PGE), respectively, to study the electrochemical performance. Compared to the homogeneous catalysis, the heterogeneous one showed a higher cathodic current and a lower over potential (about 650 mV_{NHE}). A direct reason for the performance difference in the two situations came from the presence or absence of MWCNT capable of increasing the surface area of an electrode and fast electron transfer kinetics for the CO_2 reduction process. The Re(tBu-bpy)(CO)₃Cl is another complex that has been widely studied as a homogeneous catalyst in organic solvents. When the Re(tBu-

bpy)(CO)$_3$Cl was supported on MWCNTs, the electrode could increase current densities, decrease overpotential, retain selectivity for reduction of CO_2 to CO, and allow operation in water at pH=7.3, compared to the molecular catalyst in acetonitrile solution. Current densities of 4mA/cm^2 and selectivities (FE$_{CO}$) of 99% were achieved at −0.56 V$_{RHE}$ in CO_2-saturated aqueous KHCO$_3$ solution [68].
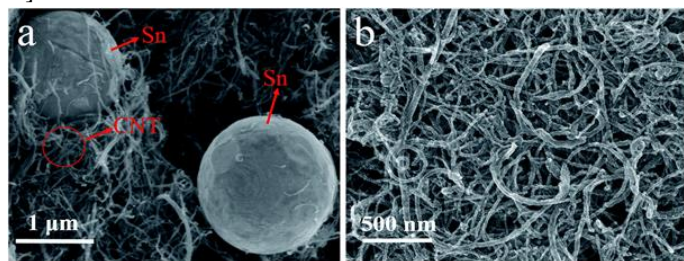

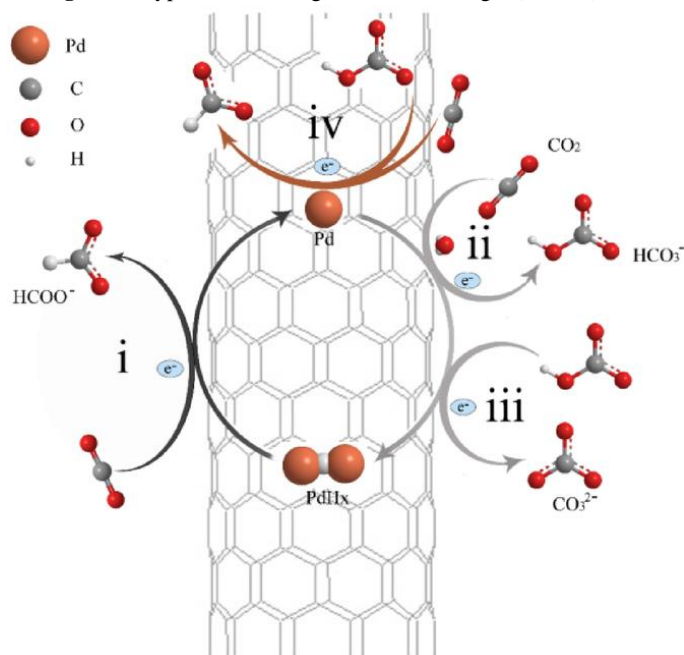**Figure 6.** Typical SEM images of Sn/CNT-Agls (a and b) [66].

Figure 7. Proposed mechanism for CO_2 electrocatalytic conversion to formate on Pd-PANI/CNT catalysts [41].

Bi is a very promising material for the selective reduction of CO_2 to formic acid in 0.5M KHCO$_3$ aqueous solution with the property of nontoxicity, negligible environmental impacts, and inexpensive price [69-71]. When combining bismuth with CNTs to prepare the catalyst, the catalytic performance can be greatly improved than pure Bi. Recently, Li *et al* [72] prepared the Bi-MWCNT-COOH/Cu catalyst by constant current electrodepositing Bi-MWCNT-COOH composite on Cu foil substrate. The as-prepared electrode showed excellent activity with high FE$_{formate}$ reaching a value 91.7% at −0.76 V$_{RHE}$ better than Bi/Cu electrode without Bi-MWCNT-COOH. In addition, the catalyst showed good stability. After 12h continuous electrolysis, the FE$_{formate}$ and current density were basically unchanged. These good performances could be attributed to the special properties of CNTs, which increased the specific surface area of the catalyst, the number of reactive sites and the conductivity of the catalyst.

Unlike the above non-precious metals, Pd is a precious metal element. But, due to the special outer-electron structure and the excellent hydrogen absorption capacity, Pd NP and its nanocomposite may be highly effective electrocatalysts for CO_2 reduction. A few noticeable studies have proved that. For example,

Pd-MWCNTs catalysts prepared by Lu *et al* [40] reduced the CO_2 to formic acid and CH$_3$COOH with a high FE (FE$_{HCOOH}$=34.5%, FE$_{CH_3COOH}$=52.3%) at −4 V$_{Ag/AgCl}$ in KHCO$_3$ electrolyte. Zhao *et al* [41] fixed Pd NPs on polyaniline-covered MWCNT surfaces to prepare the Pd-polyaniline/CNT (Pd-PANI/CNT) catalysts by using an in situ method in an ambient alenvironment. The Pd-PANI/CNT catalysts reduced the CO_2 into formate with a high FE$_{formate}$ (83%) at −0.8 V$_{SCE}$. Proposed mechanism for CO_2 electrocatalytic conversion to formate on Pd-PANI/CNT catalysts could be seen in Figure 7. The excellent catalytic performance of two catalysts mentioned above had a very important relationship to that the Pd particles were highly dispersed in carbon nanotubes with amorphous structure thereby increasing reactive sites.

Ir is precious metal material, and has high activity for ERCO$_2$. It is a commendable candidate to reduce CO_2 to the formate with a high selectivity. Researchers prepared the electrode by immobilizing Ir pincer catalyst on CNTs. They found that the electrode showed notable efficiency, selectivity, and longevity. The current density was 15 mA/cm^2 in water (0.1M NaHCO$_3$, 0.5M LiClO$_4$, 1% MeCN v/v), and the highest FE$_{formate}$ could reach as high as 96% [73].

Pt, which is also a precious metal, has inferior catalytic performance for CO_2. Hori *et al* [52] found that Pt was a good catalyst for H$_2$ evolution reaction (FE$_{H_2}$=95.7%). However, it was found that after Pt been deposited on oxygen functionalized CNT, hydrogen evolution was inhibited slightly (FE$_{H_2}$=89.8%). Based on this finding, Jimenez *et al* [42] prepared the Pt-CNT catalyst depositing Pt on CNT by using the supercritical media (supercritical CO_2). When electrochemically reducing CO_2 in gas phase, the products were formic acid (59~89%), methane (2~33%), CO (3~11%), methanol (0~1.9%), and small amounts of acetone, isopropanol, and methyl acetate. Researchers have further found that low temperature contributed to the production of methane (33%), and the high temperature was conducive to the formation of formic acid (89%).

Ag can electrochemically convert CO_2 to CO with high selectivity and current density. The development of Ag catalysts has been carried out around organometallic Ag catalysts, Ag particles with different particle sizes and so on [74]. The electrode most commonly used in the study of the catalysts is gas diffusion electrode (GDE). Because of MWCNT unique properties, it is potentially suitable as support materials for electrocatalysts. Ma *et al* [75] prepared two kinds of Ag-MWCNT catalysts by using one-step method (1) the Ag NP catalyst and MWCNTs were homogeneously distributed ("mixed" catalyst layer), (2) a layer of MWCNTs was covered with a layer of Ag catalyst ("layered" catalyst layer). Two kinds of catalysts both could reduce CO_2 into CO with a good performance, but the "mixed" layer performed best. The "mixed" layer could reduce CO_2 into CO at −3 V$_{RHE}$ with a high current density (350 mA/cm^2), FE$_{CO}$ (>95%), and energy efficiency (45%). Compared with catalyst without MWCNTs, the catalysts prepared above both had a better catalytic performance in the ERCO$_2$. And a lower charge transfer resistance was responsible for the more superior electrode performance of the "mixed" catalyst layer Ag-MWCNT catalysts.

Au as same as Ag has a decent performance for ERCO$_2$ to CO. However, on account of aggregation, Au catalyst lacks stability. To reduce the aggregation of the Au NPs and to enhance

the use of precious metals, Au NPs are often loaded on carbon materials (CMs), including CNTs, carbon black and so on, which have a high specific surface area. Feng *et al* [76] used vapor deposition to prepare Au/CNT catalyst, they found that the prepared catalyst showed high activity for CO production. After a 12h electrolysis in 0.5M NaHCO₃, the FE_{CO} was 94% at −0.50 V_{RHE}. Huan *et al* [77] anchored Au on CNTs by a layer-by-layer method, so only a few Au were used. Compared with the monodisperse Au electrode, the mass activity of the Au/CNTs was 33 times higher at −0.55V_{RHE}, and the FE_{CO} reached 70%. Moreover, surface functionalized CNTs are also used in Au-based catalysts and exhibit excellent performance. For example, Ma *et al* [78] artfully prepared a hybrid catalyst, Au NPs supported on pyridine functionalized oxidized CNTs (Au/Py-CNTs-O). And the Au/Py-CNTs-O catalyst showed good mass activity ten times than Au/CNTs-O, high FE_{CO} as high as 93% and enduring stability with little changed FE_{CO} and slight decrease in current density in the process of 10h test.

In addition to loading metal particles on the CNT, it can also load nonmetallic materials on the CNTs for efficient ERCO₂. Lu *et al* [79] developed a novel catalyst, a pyrolyzed carbon nitride (g-C₃N₄) and MWCNTs composite (g-C₃N₄/MWCNTs) which was prepared by covalently attaching graphitic carbon nitride (g-C₃N₄) onto MWCNTs with cost-effective starting materials and a simple and scalable preparation approach. The g-C₃N₄/MWCNTs reduced CO₂ to CO with a maximum FE_{CO} (60%) at an applied potential of −0.75 V_{RHE} in 0.1M CO₂-saturated KHCO₃ solution, and no significant reduction after 50 h of reaction. The catalytic activities of pristine g-C₃N₄ and MWCNTs were negligible, compared with g-C₃N₄/MWCNT whose high catalytic performance was ascribed to the active nitrogen-carbon sites formed within the g-C₃N₄/MWCNT composite, as well as significantly enlarged BET surface area and improved material conductivity.

3. GRAPHENE AS CATALYST SUPPORTING MATERIALS IN ERCO₂

Since Andre Geim and Konstantin Novoselov successfully separated the sp^2 hybrid graphene from graphite in 2004 for the first time, graphene has been widely studied and applied. It is a 2D crystal material with a honeycomb structure formed by a compact arrangement of carbon atoms in a single layer. The special structure endows graphene excellent electrical, thermal, mechanical, and optical properties [80,81]. In recent years, researchers found that graphene has huge value in the field of electrochemical CO₂ reduction. The applications of graphene and derivatives as catalyst and support material in ERCO₂ are introduced below.
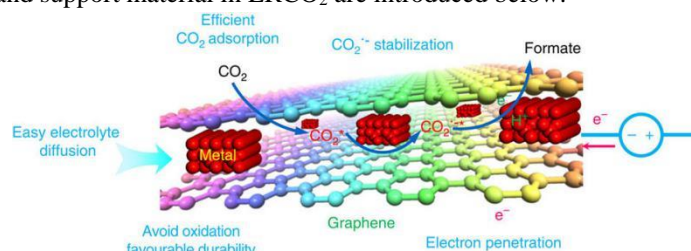

Figure 8. Schematic illustration depicts the several advantages of ultrathin metal layers confined in graphene for ERCO₂ into hydrocarbon fuels [16].

As described before, Sn has the highest chemical reactivity and selectivity in ERCO₂. However, it is less stable under the ambient conditions. In order to protect Sn from the oxidation, the researchers put forward a sandwich-like structure model (ultrathin metal layers confined in graphene). For example, Lei *et al* [16] synthesized the Sn-graphene catalyst (Sn quantum sheets confined in few-layered graphene) with the same structure and found that the Sn-graphene catalyst had more active sites to adsorb CO₂ (9 times higher than the bulk Sn). The Sn-graphene could reduce CO₂ to formate with a high current density of 21.1 mA/cm² at −1.8V_{SCE}, being 2, 2.5 and 13 times larger than the 15nm Sn NPs mixed with graphene, 15nm Sn NPs and bulk Sn, respectively. The $FE_{formate}$ was 85%, during the 50h electrolysis. Several advantages of ultrathin metal layers confined in graphene for the ERCO₂ to hydrocarbon fuels are depicted in Figure 8. Considering the nature advantages of Sn foil, which could be massively produced, directly used without complicated synthetic processes, and easily controlled to alter the size and thickness. Huang *et al* [82] prepared a single layer nitrogen-doped graphene (NG) coating Sn foil (SL-NG@Sn)

catalyst. The experiment results showed that SL-NG@Sn foil had good flexibility and could effectively reduce CO₂ to formate with outstanding FE (92.0%) at −1.0 V_{RHE} in 0.5M KHCO₃ and high formate partial current density of 21.3 mA/cm², superior to other reported Sn NPs-based catalysts, which was attributed to the synergistic effect between SL-NG and Sn foil.

Pd nanocatalysts themselves also can catalyze the ERCO₂ to produce CO [83-87], formate [88-90] and even CH₃OH [90]. To reduce costs, Pd and Cu mono- and bi-metal NPs loaded graphene catalyst were prepared using co-reduction methods by Liu *et al* [91] The results showed that the 1 wt% Pd-2 wt% Cu/graphene exhibited the best performance. The Pd/Cu-graphene catalyst had a relative positive peak potential and reduction current and the values were −1.3 $V_{Ag/AgCl}$ and −2.8 mA/cm², respectively, in CO₂ saturated KHCO₃ solution. Tao *et al* [87] recently reported a Pd/Te/FLG catalyst (FLG is few-layer graphene) for the ERCO₂ to produce CO, which doping Pd with Te enhanced the performance of the catalyst. When the ratio of Pd and Te was 1:0.05, FE_{CO} displayed the maximum 90% at −0.8 V_{RHE} and CO partial current density were 4.4 mA/cm².

There are many problems that hinder the development of the Cu-based catalyst for ERCO₂, such as, instability, poor selectivity and large reaction overpotentials. Considering the particular nature of graphene as mentioned above, it has been used as support for Cu-based catalyst. Cu is often used with rGO for the CO₂ reduction. Alves *et al* [92] fabricated the Cu/rGO catalysts for CO₂ reduction. The result showed that compared with other Cu-based electrode, the Cu/rGO had a higher current density, a lower overpotential and better stability: at −1.2 V_{NHE}. The current density observed in the Cu-NPs/rGO electrode was −0.24 mA/cm², while the same current density was reached at −1.54 V for Cu thin film. The current density obtained in the Cu-NPs/rGO at −1.54 V_{NHE} was −0.97 mA/cm², four fold higher than the Cu thin film. The Cu-NPs on rGO also exhibited better stability, preserving their catalytic activity without degradation for several hours. Recently, Hossain *et al* [93] reported a unique nanocomposite consisting of Cu NPs and rGO supported on a Cu substrate with high catalytic activity for CO₂ reduction. The optimized nanocomposite could effectively reduce CO₂ to CO, formic acid and methane with a FE of 76.6% at −0.4 V_{RHE} in a CO₂

saturated $NaHCO_3$ solution. The superior electrocatalytic activity and stability of the Cu-rGO nanocomposite achieved could be attributed to the uniformly distributed small Cu NPs on the rGO and the synergistic coupling effect of the formed nanocomposite. The electron transfer between the rGO and Cu NPs may increase localized electron concentrations, resulting in significant enhancement of the catalytic activities of the nanocomposite for the electrochemical reduction of CO_2.

Sb is rarely used for $ERCO_2$ perhaps due to that the catalytically active sites are hidden in the material. However researches find that Sb may be a suitable catalyst for the $ERCO_2$. Li *et al* [94] recently prepared a few-layer Sb nanosheet-graphene (SbNS-G) composite to reduce CO_2. They experimentally found that there was a strong electronic interaction between graphene and Sb, and that the SbNS-G had the capability to catalyze CO_2 to formate with high selectively and efficiency. The maximum $FE_{formate}$ reached up to 88.5% at -0.96 V_{RHE} in 0.5M $NaHCO_3$ solutions. At the same condition, the SbNS electrode reduced CO_2 at -1.06 V_{RHE} with a $FE_{formate}$ being 84%. Besides, the current density of the SbNS-G electrode was 1.5 and 1.6 folds higher than SbNSs and bulk Sb.

The same as Sb, Au is also rarely used in $ERCO_2$. One reason is that Au is a precious metal with expensive cost price. And the other reasons as described above, Au catalyst is lack of stability. Graphene, like carbon nanotubes, can improve the catalytic performance of the Au catalyst. Rogers *et al* [95] prepared a GNR-AuNP catalyst (gold nanoparticles embedded in a bottom-up synthesized graphene nanoribbon (GNR) matrix). The electrochemical studies showed that due to the structural and electronic properties of the GNR, the electrochemically active surface area was increased, and the overpotential of the CO_2 reduction was decreased. The onset potential of the GNR-AuNP catalyst was -0.2 V_{RHE}, the FE_{CO} was 90%, and the stability was more than 24 h. Compared with the traditional amorphous carbon AuNP supports, the catalytic output was increased by 100 times. Saquib *et al* [96] synthesized Au NPs on the rGO support (Au-rGO) and studied electrochemical performance of it. Through analyzing the values of electrochemical and impedance measurements, they found that Au-rGO had a better catalyst performance than bare Au for CO_2 reduction. The experiment also proved that the content of Au in the Au-rGO catalyst would affect the catalytic performance of the catalyst. When the Au content was less than 48.56%, with the increase of content, onset potential for CO_2 reduction was decreased. When the content was more than 48.56%, onset potential for CO_2 reduction had almost no change. For example, when the content of the Au was 35.51%, the current density was 50.95 mA/cm^2 and was the 1.65 times higher than that of rGO Au (13.72 wt%). In this work, they found that the defect sites of the rGO played a vitally significant role in CO_2 reduction by reducing the overpotential.

Mo is earth-abundant composition and has high d-electron density near the Fermi level, which is suitable active sites for CO_2 reduction. Based on this found, scarce single Mo atom loaded ultrathin NG (Mo@NG) catalyst was conducted by Huang *et al* [97]. The as-prepared electrode proved to be effective to reduction CO_2 toward formate in 4 mol% ionic liquids (ILs) with formate yield of 747 mmol/(g_{catal}·h), which was superior to conventional NG. The one of effects of NG in the catalyst was to offered proper anchor sites for stabilizing the single atom and relative endurance for a broader negative potential region thereby improving the catalyst performances for CO_2 reduction.
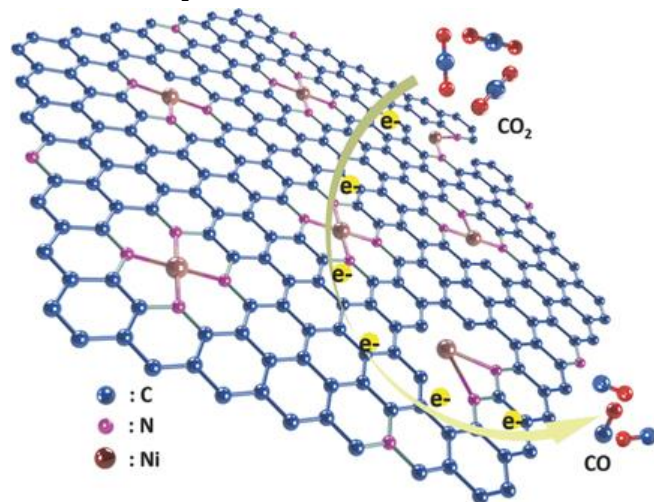

Figure 9. The structure of Ni-N-Gr [103].

Graphene materials are also used as bi-metal based catalyst carriers. For example, He *et al* [98] prepared the metal/3D-rGO electrode for CO_2 reduction. The results showed that $Pd_{0.5}$-$In_{0.5}$/3D-rGO catalyst had the best performance. The highest $FE_{formate}$ was 85.3% at -1.6 $V_{Ag/AgCl}$ in 0.5M $KHCO_3$ higher than the $Pd_{1.0}$/3D-rGO (78.6%) and $In_{1.0}$/3D- rGO (63.1%) electrode. The $FE_{formate}$ could be kept for 24h without obvious attenuation.

Graphene is also doped with heteroatoms to alter the surface properties and used as a catalyst carrier for CO_2 reduction. For example, the researchers prepared a copper NP/NG electrode consisting of Cu NPs loaded on the NG (it presents a surface of intense folds and spikes, so it called the carbon nanospikes or CNS) to reduce CO_2 to CH_3CH_2OH. The $FE_{CH_3CH_2OH}$ was 63% at -1.2 V_{RHE} in 0.1M KOH. The current density of the Cu/CNS was 5 times higher than the bare CNS and 3 times higher than the Cu [99], which was attributed to the synergistic interaction between Cu and neighboring CNS. Li *et al* [100] assembled 7nm Cu NPs on the p-NG (pyridinic-N rich graphene) at the mass ratio of 1:1 to prepare the p-NG/Cu catalyst. The p-NG itself could catalyze the CO_2 reduction to formate, but in the composite p-NG-Cu structure, the pyridinic-N functioned as a CO_2 and proton absorber, facilitating hydrogenation and carbon–carbon coupling reactions on Cu for the formation of C_2H_4. The p-NG-Cu catalyzed the reduction of CO_2 to formate (62% FE, and 97% hydrocarbon selectivity) at -0.8 V_{RHE} but to C_2H_4 (19% FE, 2.9A/g_{Cu} mass activity, and 79% hydrocarbon selectivity over other hydrocarbons) at -0.9 V_{RHE}, achieving much superior selectivity towards C_2H_4 to any other Cu-catalysts reported previously. The data showed that the combination of p-N in the p-NG and Cu NPs of a proper size (7 nm in this work) facilitated CO_2 reduction, hydrogenation and C–C coupling for the formation of C_2H_4.

Co_3O_4-based catalysts are often used in water oxidation, O_2 reduction reaction, H_2 evolution reaction. Recent studies showed that ultrathin layers of Co_3O_4 had high CO_2 reduction activity and selectivity. But there were disadvantages such as poor electron conductivity, limited surface area, and inefficient electron transfer and so on. Sekar *et al* [101] prepared a nanohybrid catalyst made up of loading of Co_3O_4 supported on NG (NG-Co_3O_4). The NG-Co_3O_4

electrode showed a higher catalytic activity compared with undoped graphene and the difference mainly came from the significant effect of NG able to obtain a controlled morphology and to facilitate a topotactic transformation during electrocatalytic conditions to CoO which resulted to be the true active phase. By the way, some cobalt complexes are also an effective composition that can be used for $ERCO_2$. For example, Wang et al [102] prepared a heterogeneous catalyst consisting of planar Co(II)-2,3-naphthalocyanine (NapCo) complexes loaded on doped graphenes including graphitic sulfoxide dopant and carboxyl dopant. The experimental results showed that NapCo supported doped graphene matrices had better good catalyst performance for CO_2 reduction to CO than Pristine NapCo without graphene supports under the identical conditions in aqueous solution. And the sulfoxide dopant was superior to carboxyl dopant with a FE for CO production up to 97%, coming from the reason that the sulfoxide dopant could further improve the electron communication between NapCo and graphene. Su et al [103] synthesized novel Ni-N-modified graphene (Ni-N-Gr) by the short-duration heat treatment of a Ni-N organo-metallic complex in the presence of GO. The HER activity of Ni-N-Gr was much lower than that of Ni-metal electrode, which was likely responsible for the high efficiency of CO formation. Compared with N-Gr and the Ni metal electrode, Ni-N-Gr exhibited a higher activity for CO formation with a high FE (90%) at –0.7 to –0.9 V_{RHE}. The structure of Ni-N-Gr can be seen in Figure 9.

4. CARBON NANOTUBES AND GRAPHENE FAMILY AS CATALYSTS IN ERCO₂

In recent years, the good chemical properties and low price of metal free catalysts have attracted the attention of the researchers. Compared with the metal-containing catalyst, the metal-free catalyst can be the next-generation, renewable materials [18].

4.1. CNT-based catalysts.

Pristine CNTs themselves actually cannot catalyze the $ERCO_2$ only if they are nitrogen-doped.[26,57,79,104-106] Most works have shown that NCNTs can reduce CO_2 to CO. For example, Sharma et al [105] found that the presence of graphitic and pyridinic nitrogen significantly decreased the overpotential (ca. ¢0.18 V) and increased the selectivity (ca. 80%) towards the formation of CO. They prepared a series of NCNTs catalysts by using different precursors (e.g. ACN, DMF, and TEA) and various growth temperatures, 750, 850, and 950°C. The NCNTs-ACN-850 (synthesized with ACN precursors at 850°C) catalyst showed the best performance. Xu et al [106] also prepared the NCNTs catalyst by a different method. MWCNTs were firstly oxidized by HNO_3 at 120, 130 or 160°C to get three types of oxidized CNTs (OCNTs). Then the washed and dried OCNTs were treated by adding poly(diallyldimethylammonium chloride) (PDDA) solution (35 wt%) with vigorous stirring, resulting in three composites (e.g. PDDA@OCNT-1, PDDA@OCNT-2 and PDDA@OCNT-3) After being filtered and washed with distilled water and ethanol and then dried for 12 h at 80°C in vacuum, they were treated via the calcination of PDDA@OCNT at 500, 700, and 900°C at air to get a series of NCNT catalysts. The highest FE_{CO} achieved was 90% and the stability was over 60 h. After 60 hours of electrolysis, the total current density and FE_{CO} were maintained at 5.8 mA/cm² and 85% at −0.9 V_{RHE}. Actually, two or more kinds of nanocarbon materials including CNTs, after being nitrogen-doped, could also be combined to be used as the catalysts. Wang et al [26] reported a low-cost, scalable nitrogen-doped nanoporous carbon/CNT (HNCM/CNT) composite membrane, which acted as the high-performance catalyst for the $ERCO_2$ to formate in 0.1M $KHCO_3$ aqueous solution ($FE_{formate}$ was 81%). Compared with the HNCM electrode, the HNCM/CNT had a more positive overpotentials and larger reduction current.

Besides CO being the main product, Zhang et al [104] also reported an $ERCO_2$ to produce formate rather than CO in CO_2-saturated aqueous $KHCO_3$ solutions using NCNTs functionalized by the polyethylenimine (PEI) as Figure 10. The highest $FE_{formate}$ achieved was 87% and the current density was 9.5 mA/cm² at −1.8 V_{SCE}. The good performance of catalysts was attributed to that the plasma treated NCNTs had a high surface.
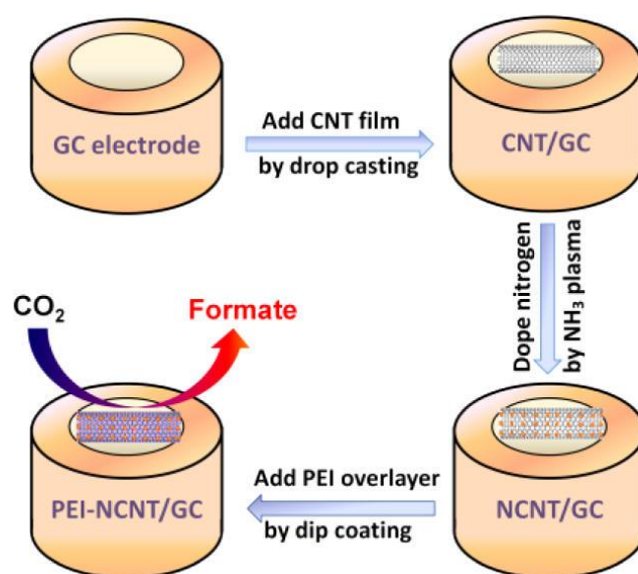

Figure 10. Fabrication of nitrogen-doped CNTs on glassy carbon electrodes with an overlayer of polyethylenimine (PEI-NCNT/GC) [104].

4.2. Graphene-based catalysts.

Like NCNTs which has a good electrochemical performance for CO_2 reduction. The graphene has a similar chemical structure to CNTs, making it equally attractive for catalytic applications. Graphene, because of its planar structure, provides a platform for a systematic independent study of catalytic activity on different N-defect structures inside carbon network [35]. Importantly, nitrogen-doping and curvature can effectively tune the activity and selectivity of graphene/CNT catalysts [38]. Therefore, the researchers began to study the catalytic performance of N-graphene to CO_2 reduction.

Wu et al [35] reported a 3D graphene foam which had nitrogen defects as a metal-free catalyst for CO_2 reduction (Figure 11). The nitrogen-doped 3D graphene foam required low onset overpotential (−0.19 V_{RHE}), and showed superior activity over Au and Ag. It reduced CO_2 to CO with a high FE_{CO} (85%) at −0.47 V_{RHE} and long stability for at least 5 h.
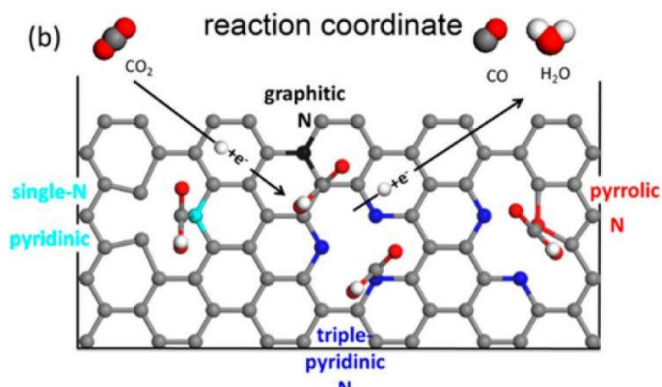
Figure 11. Schematic of N configuration and CO_2 reduction pathway [35].

Sun *et al* [107] used NG-like materials (NGM)/CP as electrodes to reduce CO_2 to methane in ionic liquids. The metal-free electrodes showed excellent activity and selectivity (FE_{CH_4}=93.5%). Moreover, with the increasing content, the FE_{CH_4} was increased. At the same time, the addition of water in the ionic liquid also had an effect on the reaction. When 3 wt% water was added in ionic liquids, the current density had double (1.42~3.26 mA/cm^2). Compared with Cu electrodes, this NGM-CP electrode showed a 6 times higher current density.
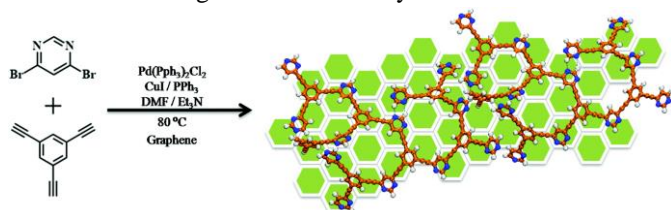

Figure 12. The one-pot, bottom-up, synthesis of the PyPOP@G. C (orange), N (blue), H (white), G (green hexagons).[108]

Wang *et al* [36] also synthesized the NG catalyst by the pyrolysis of the graphene oxide (carbon template) and melamine. When the content of the N was 5.5 atom%, the catalyst reduced CO_2 to formate in $KHCO_3$ electrolyte with a higher $FE_{formate}$ (73%). When the applied electrode potential was -0.84 V_{RHE}, the stability was 12 h, and the current density was 7.5 mA/cm^2. The researcher tried another method to improve the performance of the catalyst. Soliman *et al* [108] described a one-pot, bottom-up, pathway for constructing a novel composite material of a pyrimidine-containing porous organic polymer (PyPOP) atop graphene (PyPOP@G) sheets for application in CO_2 capture and electrocatalytic reduction. The PyPOP demonstrated an appreciable affinity toward CO_2 capture but was found to be largely insulating, hindering its usage in potential $ERCO_2$. However, its composite with graphene was found to be microporous, with a maintained affinity toward CO_2 and

furthermore demonstrated significant electrochemical activity toward CO_2 reduction (5 mA/cm^2 at -1.6 V), not observed in either of its two components separately. The one-pot, bottom-up, synthesis of the PyPOP@G is described in Figure 12.
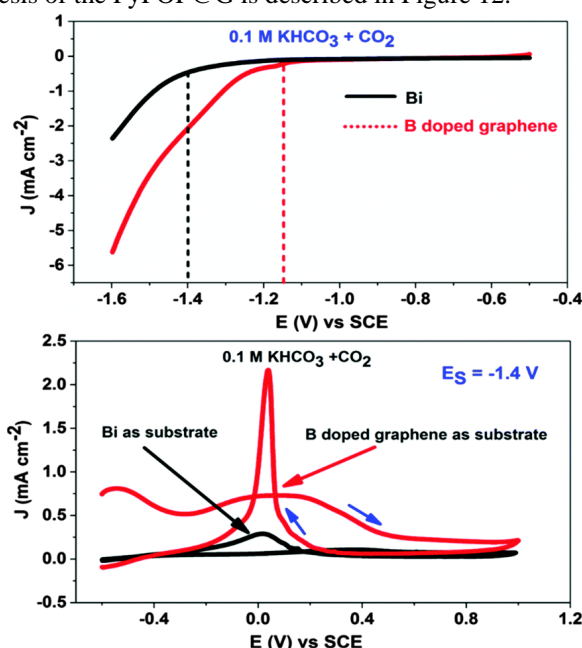

Figure 13. (a) LSV of BG (red lines) and Bi (dark lines) in 0.1 M KHCO3 in the presence of CO_2, (b) SG-TC mode: cyclic voltammetric response of the Pt UME tip probe to the product generated from the B doped graphene (red) and Bi (black) kept at a substrate potential (Es) -1.4 V in 0.1 M $KHCO_3$ saturated with CO_2; scan rate 0.05 V/s.[109]

Wu *et al* [27] prepared the nanometre-size NG quantum dots (NGQDs) used for the $ERCO_2$ into value-added chemicals at high FE, high current density and low overpotential. The NGQDs showed a high total FE up to 90% at -0.75 V_{RHE}, and had a high selectivity for ethylene and ethanol conversions (45%). The C_2 and C_3 product distribution and production rate of NGQDs catalyzing reduction of CO_2 was similar to that of Cu NP-based electrocatalysts. And the partial current densities for production of CO, C_2H_4 and C_2H_5OH (23, 46 and 21mA/cm^2 at -0.86 V_{RHE}) were similar to the commercial Cu.

Sreekanth *et al* [109] prepared a metal-free B-doped graphene (BG) to reduce CO_2 to formate in 0.1 M $KHCO_3$. Figure 13 display that compared with the Bi electrode, the B-doped graphene electrode showed a better catalyst performance for the reduction of CO_2 in 0.1 M $KHCO_3$. DFT calculations maybe can account for fact that boron-doping in graphene introduced asymmetric spin density, making it suitable for $ERCO_2$ by adsorbing on BG and not on pristine graphene and thereby undergoing reduction to formate.

5. SUMMARY, CHALLENGE AND PROPOSED RESEARCH DIRECTIONS

This paper introduces the application of CNT and graphene in the electrochemical CO_2 reduction in recent years. Because these two kinds of Carbon Materials (CMs) have the characteristics of nanometer size, high surface area and chemical stability, which has aroused the extensive attention of the researchers. Generally speaking, CMs generally have two effects in electrochemical CO_2 reduction: (1) supporting material. This takes advantage of the good conductivity of the carbon material and the better dispersion of the metal particles on it. (2) Catalyst. CMs used as catalysts are usually

doped with N or B elements. Recently, scientists have found that when carbon nanotubes or graphene are synthesized, the metal (Ni, Fe and Mn) residue on CNT and graphene will affect the catalytic performance of CMs. When the residual metals on the carbon material are washed with ultrapure nitric acid, the activity of the carbon material for the reduction of CO_2 will be greatly reduced.

There are still several technical challenges in the application of CMs for electrochemical CO_2: (1) Low CO_2 solubility. The low solubility of CO_2 is an urgent problem, which affects the efficiency

of the electrochemical CO_2 by reducing the adsorption degree of CO_2 on the surface of the electrode; (2) Low catalyst activity. It can be seen from the above that for every single type of catalyst developed in the literature, the overpotential for CO_2 electroreduction is normally too high, indicating that these catalysts' activities are still not good enough for practical applications in terms of energy efficiency; (3) Low product selectivity. For the majority of the carbon-based catalysts discussed above, even if the activity is high, the selectivity is not good enough. In addition to the target product, there will be hydrogen and other products. And some carbon-based catalysts which have a high selectivity are suffered from low stability. So, if we want to promote the large-scale application of electrochemical CO_2, we can change the way of application of the product. For instance, if the products are H_2 and CO, we can change the ratio of H_2 and CO and use the product as syngas.

Because of the good performance of CNTs and graphene, they have been widely developed in recent years. A large part of them is not used in the field of electrochemical reduction CO_2. For example, (i) different forms of CMs: the catalytic performance of the catalyst is affected by the morphology. The morphology of the catalyst is different, and the catalytic performance will vary. Fiber-like CNT, direct spun CNT fiber, 3D graphene. (ii) The properties of different elements doped CMs are also different. In addition to the common nitrogen-doping, there are Fe-N-doped CNTs, B-O-dually doped MWCNTs, N-S-codoped graphene and so on. (iii) Generally, alloy materials will improve the properties of metal materials. The catalysts which are synthesized with alloy and CMs can improve the catalytic performance of the catalyst. (iiii) Recent studies have found that some organic compounds, such as MOF, have high activity for the reduction of CO_2 reduction. But the organic compounds itself has no good electrical conductivity. The catalytic performance of organic compounds can be further improved if the catalyst is synthesized with CMs and organic compounds.

6. CONCLUSIONS

$ERCO_2$ to value-added chemical and low carbon fuels has been recognized as an economic, environment-friendly and easily scale-up technology to efficiently deal with the problems of energy dilemma and greenhouse effect. For this purpose, efficient and robust catalysts will play important roles in getting down the reaction overpotential and reducing energy consumption in the process. In this paper, we review the applications of CNTs and graphene as support materials and even catalysts for $ERCO_2$, which have attracted wide attentions in the past decades. When these two novel carbon materials acted as catalyst supports, more perfect performances of catalysts, such as higher FE, product selectivity and stability for $ERCO_2$, were popularly achieved compared with that of simple catalyst materials. it can be attributed to nanostructures and characteristics of CNTs and graphene, which are helpful for increasing the specific surface area and the active sites of loaded catalysts, resulting in enhanced the catalytic performances. When both novel carbon materials are doped with heteroatoms such as nitrogen and sulfur, they can act as the metal-free catalysts with significant electrochemical activity toward CO_2 reduction. Consequently, Both CNTs and graphene are promising materials for boosting the $ERCO_2$. To make large utilization of carbon materials in $ERCO_2$, further work is needed for some key problems such as the effects of heteroatom doping and structural defect.

7. REFERENCES

1. Kumar, B.; Llorente, M.; Froehlich, J.; Dang, T.; Sathrum, A.; Kubiak, C.P. Photochemical and Photoelectrochemical Reduction of CO_2. In: *Annual Review of Physical Chemistry.* Johnson, M.A.; Martinez, T.J.; Volume 63. Eds. 2012; pp. 541-569, https://doi.org/10.1146/annurev-physchem-032511-143759.

2. Costentin, C.; Robert, M.; Saveant, J.M. Catalysis of the electrochemical reduction of carbon dioxide. *Chemical Society Reviews* **2013**, *42*, 2423-2436, https://doi.org/10.1039/c2cs35360a.

3. Qiao, J.; Liu, Y.; Hong, F.; Zhang, J. A review of catalysts for the electroreduction of carbon dioxide to produce low-carbon fuels. *Chemical Society Reviews* **2014**, *43*, 631-675, https://doi.org/10.1039/c3cs60323g.

4. Wang, W.H.; Himeda, Y.; Muckerman, J.T.; Manbeck, G.F.; Fujita, E. CO_2 Hydrogenation to Formate and Methanol as an Alternative to Photo- and Electrochemical CO_2 Reduction. *Chemical Reviews* **2015**, *115*, 12936-12973, https://doi.org/10.1021/acs.chemrev.5b00197.

5. Francke, R.; Schille, B.; Roemelt, M. Homogeneously Catalyzed Electroreduction of Carbon Dioxide-Methods, Mechanisms, and Catalysts. *Chemical Reviews* **2018**, *118*, 4631-4701, https://doi.org/10.1021/acs.chemrev.7b00459.

6. Genovese, C.; Ampelli, C.; Perathoner, S.; Centi, G. Electrocatalytic conversion of CO_2 to liquid fuels using nanocarbon-based electrodes. *Journal of Energy Chemistry* **2013**, *22*, 202-213, https://doi.org/10.1016/S2095-4956(13)60026-1.

7. Arico, A.S.; Bruce, P.; Scrosati, B.; Tarascon, J.M.; van Schalkwijk, W. Nanostructured materials for advanced energy conversion and storage devices. *Nature materials* **2005**, *4*, 366-377, https://doi.org/10.1038/nmat1368.

8. Su, D.S.; Schlogl, R. Nanostructured carbon and carbon nanocomposites for electrochemical energy storage applications. *ChemSusChem* **2010**, *3*, 136-168, https://doi.org/10.1002/cssc.200900182.

9. Su, D.S.; Zhang, J.; Frank, B.; Thomas, A.; Wang, X.; Paraknowitsch, J.; Schlogl, R. Metal-free heterogeneous catalysis for sustainable chemistry. *ChemSusChem* **2010**, *3*, 169-180, https://doi.org/10.1002/cssc.200900180.

10. Ge, P.; Scanlon, M.D.; Peljo, P.; Bian, X.; Vubrel, H.; O'Neill, A.; Coleman, J.N.; Cantoni, M.; Hu, X.; Kontturi, K.; Liu, B.H.; Girault, H.H. Hydrogen evolution across nano-Schottky junctions at carbon supported MoS_2 catalysts in biphasic liquid systems. *Chemical Communications* **2012**, *48*, 6484-6486, https://doi.org/10.1039/c2cc31398g.

11. Qiao, J.L.; Xu, L.; Liu, Y.Y.; Xu, P.; Shi, J.J.; Liu, S.Y.; Tian, B.L. Carbon-supported co-pyridine as non-platinum cathode catalyst for alkaline membrane fuel cells. *Electrochimica Acta* **2013**, *96*, 298-305, https://doi.org/10.1016/j.electacta.2013.02.030.

12. Zheng, Y.; Jiao, Y.; Qiao, S.Z. Engineering of Carbon-Based Electrocatalysts for Emerging Energy Conversion: From Fundamentality to Functionality. *Advanced Materials* **2015**, *27*, 5372-5378, https://doi.org/10.1002/adma.201500821.

13. Pan, Y.; Hu, W.H.; Liu, D.P.; Liu, Y.Q.; Liu, C.G. Carbon

nanotubes decorated with nickel phosphide nanoparticles as efficient nanohybrid electrocatalysts for the hydrogen evolution reaction. *Journal of Materials Chemistry A* **2015**, *3*, 13087-13094, https://doi.org/10.1039/c5ta02128f.

14. Liu, L.; Zhu, Y.P.; Su, M.; Yuan, Z.Y. Metal-Free Carbonaceous Materials as Promising Heterogeneous Catalysts. *ChemCatChem* **2015**, *7*, 2765-2787, https://doi.org/10.1002/cctc.201500350.

15. Tang, P.; Hu, G.; Li, M.Z.; Ma, D. Graphene-Based Metal-Free Catalysts for Catalytic Reactions in the Liquid Phase. *ACS Catalysis* **2016**, *6*, 6948-6958, https://doi.org/10.1021/acscatal.6b01668.

16. Lei, F.; Liu, W.; Sun, Y.; Xu, J.; Liu, K.; Liang, L.; Yao, T.; Pan, B.; Wei, S.; Xie, Y. Metallic tin quantum sheets confined in graphene toward high-efficiency carbon dioxide electroreduction. *Nature Communications* **2016**, *7*, 12697, https://doi.org/10.1038/ncomms12697.

17. Luc, W.; Collins, C.; Wang, S.; Xin, H.; He, K.; Kang, Y.; Jiao, F. Ag-Sn Bimetallic Catalyst with a Core-Shell Structure for CO$_2$ Reduction. *Journal of the American Chemical Society* **2017**, *139*, 1885-1893, https://doi.org/10.1021/jacs.6b10435.

18. Vasileff, A.; Zheng, Y.; Qiao, S.Z. Carbon Solving Carbon's Problems: Recent Progress of Nanostructured Carbon-Based Catalysts for the Electrochemical Reduction of CO$_2$. *Advanced Energy Materials* **2017**, *7*, https://doi.org/10.1002/aenm.201700759.

19. Liu, T.F.; Ali, S.; Lian, Z.; Li, B.; Su, D.S. CO$_2$ electoreduction reaction on heteroatom-doped carbon cathode materials. *Journal of Materials Chemistry A* **2017**, *5*, 21596-21603, https://doi.org/10.1039/c7ta06674k.

20. Xie, J.; Zhao, X.; Wu, M.; Li, Q.; Wang, Y.; Yao, J. Metal-Free Fluorine-Doped Carbon Electrocatalyst for CO$_2$ Reduction Outcompeting Hydrogen Evolution. *Angewandte Chemie International Edition* **2018**, *57*, 9640-9644, https://doi.org/10.1002/anie.201802055.

21. Yuan, J.; Zhi, W.Y.; Liu, L.; Yang, M.P.; Wang, H.; Lu, J.X. Electrochemical reduction of CO$_2$ at metal-free N-functionalized graphene oxide electrodes. *Electrochimica Acta* **2018**, *282*, 694-701, https://doi.org/10.1016/j.electacta.2018.06.107.

22. Yamamoto, T.; Tryk, D.A.; Hashimoto, K.; Fujishima, A.; Okawa, M. Electrochemical Reduction of CO$_2$ in the Micropores of Activated Carbon Fibers. *Journal of the Chemical Society* **2000**, *147*, 3393, https://doi.org/10.1149/1.1393911.

23. Ikemiya, N.; Natsui, K.; Nakata, K.; Einaga, Y. Long-Term Continuous Conversion of CO$_2$ to Formic Acid Using Boron-Doped Diamond Electrodes. *ACS Sustainable Chemistry & Engineering* **2018**, *6*, 8108-8112, https://doi.org/10.1021/acssuschemeng.8b00793.

24. Roy, N.; Shibano, Y.; Terashima, C.; Katsumata, K.; Nakata, K.; Kondo, T.; Yuasa, M.; Fujishima, A. Ionic-Liquid-Assisted Selective and Controlled Electrochemical CO$_2$ Reduction at Cu-Modified Boron-Doped Diamond Electrode. *ChemElectroChem* **2016**, *3*, 1044-1047, https://doi.org/10.1002/celc.201600105.

25. Jiwanti, P.K.; Natsui, K.; Nakata, K.; Einaga, Y. The electrochemical production of C-2/C-3 species from carbon dioxide on copper-modified boron-doped diamond electrodes. *Electrochimica Acta* **2018**, *266*, 414-419, https://doi.org/10.1016/j.electacta.2018.02.041.

26. Wang, H.; Jia, J.; Song, P.; Wang, Q.; Li, D.; Min, S.; Qian, C.; Wang, L.; Li, Y.F.; Ma, C.; Wu, T.; Yuan, J.; Antonietti, M.; Ozin, G.A. Efficient Electrocatalytic Reduction of CO$_2$ by Nitrogen-Doped Nanoporous Carbon/Carbon Nanotube Membranes: A Step Towards the Electrochemical CO$_2$ Refinery. *Angewandte Chemie International Edition* **2017**, *56*, 7847-7852, https://doi.org/10.1002/anie.201703720.

27. Wu, J.; Ma, S.; Sun, J.; Gold, J.I.; Tiwary, C.; Kim, B.; Zhu, L.; Chopra, N.; Odeh, I.N.; Vajtai, R.; Yu, A.Z.; Luo, R.; Luo, J.;

Ding, G.; Kenis, P.J.A.; Ajayan, P.M. A metal-free electrocatalyst for carbon dioxide reduction to multi-carbon hydrocarbons and oxygenates. *Nature Communications* **2016**, *7*, https://doi.org/10.1038/ncomms13869.

28. Zou, X.L.; Liu, M.J.; Wu, J.J.; Ajayan, P.M.; Li, J.; Liu, B.L.; Yakobson, B.I. How Nitrogen-Doped Graphene Quantum Dots Catalyze Electroreduction of CO$_2$ to Hydrocarbons and Oxygenates. *ACS Catalysis* **2017**, *7*, 6245-6250, https://doi.org/10.1038/ncomms13869.

29. Fu, J.; Wang, Y.; Liu, J.; Huang, K.; Chen, Y.; Li, Y.; Zhu, J.-J. Low Overpotential for Electrochemically Reducing CO$_2$ to CO on Nitrogen-Doped Graphene Quantum Dots-Wrapped Single-Crystalline Gold Nanoparticles. *ACS Energy Letters* **2018**, *3*, 946-951, https://doi.org/10.1021/acsenergylett.8b00261.

30. Wu, J.; Yadav, R.M.; Liu, M.; Sharma, P.P.; Tiwary, C.S.; Ma, L.; Zou, X.; Zhou, X.D.; Yakobson, B.I.; Lou, J., et al. Achieving Highly Efficient, Selective, and Stable CO$_2$ Reduction on Nitrogen-Doped Carbon Nanotubes. *ACS Nano,* **2015**, *9*, 5364-5371, https://doi.org/10.1021/acsnano.5b01079.

31. Sharma, P.P.; Wu, J.; Yadav, R.M.; Liu, M.; Wright, C.J.; Tiwary, C.S.; Yakobson, B.I.; Lou, J.; Ajayan, P.M.; Zhou, X.D. Nitrogen-Doped Carbon Nanotube Arrays for High-Efficiency Electrochemical Reduction of CO$_2$: On the Understanding of Defects, Defect Density, and Selectivity. *Angewandte Chemie International Edition* **2015**, *54*, 13701-13705, https://doi.org/10.1002/ange.201506062.

32. Malik, M.I.; Malaibari, Z.O.; Atieh, M.; Abussaud, B. Electrochemical reduction of CO$_2$ to methanol over MWCNTs impregnated with Cu$_2$O. *Chemical Engineering Science* **2016**, *152*, 468-477, https://doi.org/10.1016/j.ces.2016.06.035.

33. Tuci, G.; Rossin, A.; Luconi, L.; Pham-Huu, C.; Cicchi, S.; Ba, H.; Giambastiani, G. Pyridine-decorated carbon nanotubes as a metal-free heterogeneous catalyst for mild CO$_2$ reduction to methanol with hydroboranes. *Catalysis Science & Technology* **2017**, *7*, 5833-5837, https://doi.org/10.1039/c7cy01772c.

34. Cui, X.Q.; Pan, Z.Y.; Zhang, L.J.; Peng, H.S.; Zheng, G.F. Selective Etching of Nitrogen-Doped Carbon by Steam for Enhanced Electrochemical CO$_2$ Reduction. *Advanced Energy Materials* **2017**, *7*, https://doi.org/10.1002/aenm.201701456.

35. Wu, J.; Liu, M.; Sharma, P.P.; Yadav, R.M.; Ma, L.; Yang, Y.; Zou, X.; Zhou, X.D.; Vajtai, R.; Yakobson, B.I.; Lou, J.; Ajayan, P.M. Incorporation of Nitrogen Defects for Efficient Reduction of CO$_2$ via Two-Electron Pathway on Three-Dimensional Graphene Foam. *Nano Letters* **2016**, *16*, 466-470, https://doi.org/10.1021/acs.nanolett.5b04123.

36. Wang, H.X.; Chen, Y.B.; Hou, X.L.; Ma, C.Y.; Tan, T.W. Nitrogen-doped graphenes as efficient electrocatalysts for the selective reduction of carbon dioxide to formate in aqueous solution. *Green Chemistry* **2016**, *18*, 3250-3256, https://doi.org/10.1039/c6gc00410e.

37. Liu, Y.; Zhao, J.; Cai, Q. Pyrrolic-nitrogen doped graphene: a metal-free electrocatalyst with high efficiency and selectivity for the reduction of carbon dioxide to formic acid: a computational study. *Physical Chemistry Chemical Physics,* **2016**, *18*, 5491-5498, https://doi.org/10.1039/c5cp07458d.

38. Chai, G.L.; Guo, Z.X. Highly effective sites and selectivity of nitrogen-doped graphene/CNT catalysts for CO$_2$ electrochemical reduction. *Chemical Science* **2016**, *7*, 1268-1275, https://doi.org/10.1039/c5sc03695j.

39. Siahrostami, S.; Jiang, K.; Karamad, M.; Chan, K.R.; Wang, H.T.; Norskov, J. Theoretical Investigations into Defected Graphene for Electrochemical Reduction of CO$_2$. *ACS Sustainable Chemistry & Engineering* **2017**, *5*, 11080-11085, https://doi.org/10.1021/acssuschemeng.7b03031.

40. Lu, G.; Wang, H.; Bian, Z.; Liu, X. Electrochemical reduction of CO$_2$ to organic acids by a Pd-MWNTs gas-diffusion electrode in aqueous medium. *Scientific World Journal* **2013**, *2013*,

https://doi.org/10.1155/2013/424617.

41. Zhao, C.C.; Yin, Z.S.; Wang, J.L. Efficient Electrochemical Conversion of CO₂ to HCOOH Using Pd-polyaniline/CNT Nanohybrids Prepared in Situ. *ChemElectroChem* **2015**, *2*, 1974-1982, https://doi.org/10.1002/celc.201500328.

42. Jimenez, C.; Garcia, J.; Camarillo, R.; Martinez, F.; Rincon, J. Electrochemical CO₂ Reduction to Fuels Using Pt/CNT Catalysts Synthesized in Supercritical Medium. *Energy & Fuels* **2017**, *31*, 3038-3046, https://doi.org/10.1021/acs.energyfuels.6b03017.

43. Walsh, J.J.; Neri, G.; Smith, C.L.; Cowan, A.J. Electrocatalytic CO₂ reduction with a membrane supported manganese catalyst in aqueous solution. *Chemical Communications* **2014**, *50*, 12698-12701, https://doi.org/10.1039/c4cc06404f.

44. Bashir, S.M.; Hossain, S.S.; Rahman, S.U.; Ahmed, S.; Hossain, M.M. NiO/MWCNT Catalysts for Electrochemical Reduction of CO₂. *Electrocatalysis-US* **2015**, *6*, 544-553, https://doi.org/10.1007/s12678-015-0270-1.

45. Hossain, S.S.; Rahman, S.U.; Ahmed, S. Electrochemical Reduction of Carbon Dioxide over CNT-Supported Nanoscale Copper Electrocatalysts. *Journal of Nanomaterials* **2014**, https://doi.org/10.1155/2014/374318.

46. Bashir, S.; Hossain, S.S.; Rahman, S.U.; Ahmed, S.; Al-Ahmed, A.; Hossain, M.M. Electrocatalytic reduction of carbon dioxide on SnO₂/MWCNT in aqueous electrolyte solution. *Journal of CO₂ Utilization* **2016**, *16*, 346-353, https://doi.org/10.1016/j.jcou.2016.09.002.

47. Riplinger, C.; Carter, E.A. Influence of Weak Bronsted Acids on Electrocatalytic CO₂ Reduction by Manganese and Rhenium Bipyridine Catalysts. *ACS Catalysis* **2015**, *5*, 900-908, https://doi.org/10.1021/cs501687n.

48. Bourrez, M.; Molton, F.; Chardon-Noblat, S.; Deronzier, A. [Mn(bipyridyl)(CO)₃Br]: an abundant metal carbonyl complex as efficient electrocatalyst for CO₂ reduction. *Angewandte Chemie International Edition* **2011**, *50*, 9903-9906, https://doi.org/10.1002/anie.201103616.

49. Smieja, J.M.; Sampson, M.D.; Grice, K.A.; Benson, E.E.; Froehlich, J.D.; Kubiak, C.P. Manganese as a substitute for rhenium in CO₂ reduction catalysts: the importance of acids. *Inorganic Chemistry* **2013**, *52*, 2484-2491, https://doi.org/10.1021/ic302391u.

50. Sampson, M.D.; Nguyen, A.D.; Grice, K.A.; Moore, C.E.; Rheingold, A.L.; Kubiak, C.P. Manganese catalysts with bulky bipyridine ligands for the electrocatalytic reduction of carbon dioxide: eliminating dimerization and altering catalysis. *Journal of the American Chemical Society* **2014**, *136*, 5460-5471, https://doi.org/10.1021/ja501252f.

51. Sato, S.; Saita, K.; Sekizawa, K.; Maeda, S.; Morikawa, T. Low-Energy Electrocatalytic CO₂ Reduction in Water over Mn-Complex Catalyst Electrode Aided by a Nanocarbon Support and K⁺ Cations. *ACS Catalysis* **2018**, *8*, 4452-4458, https://doi.org/10.1021/acscatal.8b01068.

52. Hori, Y.; Wakebe, H.; Tsukamoto, T.; Koga, O. Electrocatalytic process of CO selectivity in electrochemical reduction of CO₂ at metal electrodes in aqueous media. *Electrochimica Acta* **1994**, *39*, 1833-1839, https://doi.org/10.1016/0013-4686(94)85172-7.

53. Genovese, C.; Ampelli, C.; Perathoner, S.; Centi, G. Electrocatalytic conversion of CO₂ on carbon nanotube-based electrodes for producing solar fuels. *Journal of Catalysis* **2013**, *308*, 237-249, https://doi.org/10.1016/j.jcat.2013.08.026.

54. Zhao, H.Z.; Chang, Y.Y.; Liu, C. Electrodes modified with iron porphyrin and carbon nanotubes: application to CO₂ reduction and mechanism of synergistic electrocatalysis. *Journal of Solid State Electrochemistry* **2013**, *17*, 1657-1664, https://doi.org/10.1007/s10008-013-2027-1.

55. Maurin, A.; Robert, M. Catalytic CO₂-to-CO conversion in water by covalently functionalized carbon nanotubes with a molecular iron catalyst. *Chemical Communications* **2016**, *52*, 12084-12087, https://doi.org/10.1039/c6cc05430g.

56. Maurin, A.; Robert, M. Noncovalent Immobilization of a Molecular Iron-Based Electrocatalyst on Carbon Electrodes for Selective, Efficient CO₂-to-CO Conversion in Water. *Journal of the American Chemical Society* **2016**, *138*, 2492-2495, https://doi.org/10.1021/jacs.5b12652.

57. Jia, J.C.; Yang, H.J.; Wang, G.X.; Huang, P.; Cai, P.W.; Wen, Z.H. Fe/Fe₃C Nanoparticles Embedded in Nitrogen-Doped Carbon Nanotubes as Multifunctional Electrocatalysts for Oxygen Catalysis and CO₂ Reduction. *ChemElectroChem* **2018**, *5*, 471-477, https://doi.org/10.1002/celc.201701179.

58. Dempsey, J.L.; Brunschwig, B.S.; Winkler, J.R.; Gray, H.B. Hydrogen evolution catalyzed by cobaloximes. *Accounts of Chemical Research* **2009**, *42*, 1995-2004, https://doi.org/10.1021/ar900253e.

59. Aoi, S.; Mase, K.; Ohkubo, K.; Fukuzumi, S. Selective electrochemical reduction of CO₂ to CO with a cobalt chlorin complex adsorbed on multi-walled carbon nanotubes in water. *Chemical Communications* **2015**, *51*, 10226-10228, https://doi.org/10.1039/c5cc03340c.

60. Murata, A.; Hori, Y. Product Selectivity Affected by Cationic Species in Electrochemical Reduction of CO₂ and CO at a Cu Electrode. *Bulletin of the Chemical Society of Japan* **1991**, *64*, 123-127, https://doi.org/10.1246/bcsj.64.123.

61. Baturina, O.A.; Lu, Q.; Padilla, M.A.; Xin, L.; Li, W.Z.; Serov, A.; Artyushkova, K.; Atanassov, P.; Xu, F.; Epshteyn, A.; Brintlinger, T.; Schuette, M.; Collins, G.E. CO₂ Electroreduction to Hydrocarbons on Carbon-Supported Cu Nanoparticles. *ACS Catalysis* **2014**, *4*, 3682-3695, https://doi.org/10.1021/cs500537y.

62. Koo, Y.; Malik, R.; Alvarez, N.; White, L.; Shanov, V.N.; Schulz, M.; Collins, B.; Sankar, J.; Yun, Y. Aligned carbon nanotube/copper sheets: a new electrocatalyst for CO₂ reduction to hydrocarbons. *RSC Advances* **2014**, *4*, 16362-16367, https://doi.org/10.1039/c4ra00618f.

63. Marepally, B.C.; Ampelli, C.; Genovese, C.; Tavella, F.; Veyre, L.; Quadrelli, E.A.; Perathoner, S.; Centi, G. Role of small Cu nanoparticles in the behaviour of nanocarbon-based electrodes for the electrocatalytic reduction of CO₂. *Journal of CO₂ Utilization* **2017**, *21*, 534-542, https://doi.org/10.1016/j.jcou.2017.08.008.

64. Genovese, C.; Ampelli, C.; Perathoner, S.; Centi, G. Mechanism of C-C bond formation in the electrocatalytic reduction of CO₂ to acetic acid. A challenging reaction to use renewable energy with chemistry. *Green Chemistry* **2017**, *19*, 2406-2415, https://doi.org/10.1039/c6gc03422e.

65. Huo, S.; Weng, Z.; Wu, Z.; Zhong, Y.; Wu, Y.; Fang, J.; Wang, H. Coupled Metal/Oxide Catalysts with Tunable Product Selectivity for Electrocatalytic CO₂ Reduction. *ACS Applied Materials & Interfaces* **2017**, *9*, 28519-28526, https://doi.org/10.1021/acsami.7b07707.

66. Chen, Z.P.; Yao, S.Y.; Liu, L.C. 3D hierarchical porous structured carbon nanotube aerogel-supported Sn spheroidal particles: an efficient and selective catalyst for electrochemical reduction of CO₂ to formate. *Journal of Materials Chemistry A* **2017**, *5*, 24651-24656, https://doi.org/10.1039/c7ta07495f.

67. Rezaei, B.; Mokhtarianpour, M.; Ensafi, A.A.; Hadadzadeh, H.; Shakeni, J. Electrocatalytic reduction of CO₂ using the dinuclear rhenium(I) complex [ReCl(CO)₃(μ-tptzH)Re(CO)₃]. *Polyhedron* **2015**, *101*, 160-164, https://doi.org/10.1016/j.poly.2015.08.014.

68. Zhanaidarova, A.; Jones, S.C.; Despagnet-Ayoub, E.; Pimentel, B.R.; Kubiak, C.P. Re(tBu-bpy)(CO)₃Cl Supported on Multi-Walled Carbon Nanotubes Selectively Reduces CO₂ in Water. *Journal of the American Chemical Society,* **2019**, *141*, 17270-17277, https://doi.org/10.1021/jacs.9b08445.

69. Park, J.Y.; Kim, S.; Hong, D.M.; Lim, J.W.; Yoo, C.J.; Dong, W.J.; Lee, J.L. The Effect of Pulse Electrodeposition of Bismuth on Electrochemical Reduction of Carbon Dioxide to Formate. *Electronic Materials Letters* **2019**, *15*, 454-461, https://doi.org/10.1007/s13391-019-00145-8.

70. Oh, W.; Rhee, C.K.; Han, J.W.; Shong, B. Atomic and Molecular Adsorption on the Bi(111) Surface: Insights into Catalytic CO_2 Reduction. *Journal of Physical Chemistry C,* **2018**, *122*, 23084-23090, https://doi.org/10.1021/acs.jpcc.8b07865.

71. DiMeglio, J.L.; Rosenthal, J. Selective conversion of CO_2 to CO with high efficiency using an inexpensive bismuth-based electrocatalyst. *Journal of the American Chemical Society* **2013**, *135*, 8798-8801, https://doi.org/10.1021/ja4033549.

72. Li, Q.; Zhang, X.; Zhou, X.; Li, Q.; Wang, H.; Yi, J.; Liu, Y.; Zhang, J. Simply and effectively electrodepositing Bi-MWCNT-COOH composite on Cu electrode for efficient electrocatalytic CO_2 reduction to produce HCOOH. *Journal of CO_2 Utilization* **2020**, *37*, 106-112, https://doi.org/10.1016/j.jcou.2019.12.003.

73. Kang, P.; Zhang, S.; Meyer, T.J.; Brookhart, M. Rapid selective electrocatalytic reduction of carbon dioxide to formate by an iridium pincer catalyst immobilized on carbon nanotube electrodes. *Angewandte Chemie International Edition* **2014**, *53*, 8709-8713, https://doi.org/10.1002/anie.201310722.

74. Tornow, C.E.; Thorson, M.R.; Ma, S.; Gewirth, A.A.; Kenis, P.J. Nitrogen-based catalysts for the electrochemical reduction of CO_2 to CO. *Journal of the American Chemical Society* **2012**, *134*, 19520-19523, https://doi.org/10.1021/ja308217w.

75. Ma, S.C.; Luo, R.; Gold, J.I.; Yu, A.Z.; Kim, B.; Kenis, P.J.A. Carbon nanotube containing Ag catalyst layers for efficient and selective reduction of carbon dioxide. *Journal of Materials Chemistry A* **2016**, *4*, 8573-8578, https://doi.org/10.1039/c6ta00427j.

76. Feng, X.; Jiang, K.; Fan, S.; Kanan, M.W. Grain-boundary-dependent CO_2 electroreduction activity. *Journal of the American Chemical Society* **2015**, *137*, 4606-4609, https://doi.org/10.1021/ja5130513.

77. Huan, T.N.; Prakash, P.; Simon, P.; Rousse, G.; Xu, X.; Artero, V.; Gravel, E.; Doris, E.; Fontecave, M. CO_2 Reduction to CO in Water: Carbon Nanotube-Gold Nanohybrid as a Selective and Efficient Electrocatalyst. *ChemSusChem* **2016**, *9*, 2317-2320, https://doi.org/10.1002/cssc.201600597.

78. Ma, Z.; Lian, C.; Niu, D.; Shi, L.; Hu, S.; Zhang, X.; Liu, H. Enhancing CO_2 Electroreduction with Au/Pyridine/Carbon Nanotubes Hybrid Structures. *ChemSusChem* **2019**, *12*, 1724-1731, https://doi.org/10.1002/cssc.201802940.

79. Lu, X.; Tan, T.H.; Ng, Y.H.; Amal, R. Highly Selective and Stable Reduction of CO_2 to CO by a Graphitic Carbon Nitride/Carbon Nanotube Composite Electrocatalyst. *Chemistry* **2016**, *22*, 11991-11996, https://doi.org/10.1002/chem.201601674.

80. Novoselov, K.S.; Geim, A.K.; Morozov, S.V.; Jiang, D.; Zhang, Y.; Dubonos, S.V.; Grigorieva, I.V.; Firsov, A.A. Electric field effect in atomically thin carbon films. *Science* **2004**, *306*, 666-669, https://doi.org/10.1126/science.1102896.

81. Geim, A.K.; Novoselov, K.S. The rise of graphene. *Nature Materials* **2007**, *6*, 183-191, https://doi.org/10.1038/nmat1849.

82. Huang, J.; Guo, X.; Wei, Y.; Hu, Q.; Yu, X.; Wang, L. A renewable, flexible and robust single layer nitrogen-doped graphene coating Sn foil for boosting formate production from electrocatalytic CO_2 reduction. *Journal of CO_2 Utilization* **2019**, *33*, 166-170, https://doi.org/10.1016/j.jcou.2019.05.026.

83. Gao, D.; Zhou, H.; Wang, J.; Miao, S.; Yang, F.; Wang, G.; Wang, J.; Bao, X. Size-dependent electrocatalytic reduction of CO_2 over Pd nanoparticles. *Journal of the American Chemical Society* **2015**, *137*, 4288-4291, https://doi.org/10.1021/jacs.5b00046.

84. Kortlever, R.; Peters, I.; Balemans, C.; Kas, R.; Kwon, Y.; Mul, G.; Koper, M.T. Palladium-gold catalyst for the electrochemical reduction of CO_2 to C_1-C_5 hydrocarbons. *Chemical Communications* **2016**, *52*, 10229-10232, https://doi.org/10.1039/c6cc03717h.

85. Huang, H.; Jia, H.; Liu, Z.; Gao, P.; Zhao, J.; Luo, Z.; Yang, J.; Zeng, J. Understanding of Strain Effects in the Electrochemical Reduction of CO_2 : Using Pd Nanostructures as an Ideal Platform. *Angew Chem Int Edit* **2017**, *56*, 3594-3598, https://doi.org/10.1002/anie.201612617.

86. Zhu, W.; Zhang, L.; Yang, P.; Hu, C.; Luo, Z.; Chang, X.; Zhao, Z.J.; Gong, J. Low-Coordinated Edge Sites on Ultrathin Palladium Nanosheets Boost Carbon Dioxide Electroreduction Performance. *Angewandte Chemie International Edition* **2018**, *57*, 11544-11548, https://doi.org/10.1002/anie.201806432.

87. Tao, H.; Sun, X.; Back, S.; Han, Z.; Zhu, Q.; Robertson, A.W.; Ma, T.; Fan, Q.; Han, B.; Jung, Y,; Sun, Z. Doping palladium with tellurium for the highly selective electrocatalytic reduction of aqueous CO_2 to CO. *Chemical Science* **2018**, *9*, 483-487, https://doi.org/10.1039/c7sc03018e.

88. Lu, G.; Wang, H.; Bian, Z.Y.; Liu, X. Electrocatalytic reduction of CO_2 to formic acid on palladium-graphene nanocomposites gas-diffusion electrode. *Journal of Nanoscience and Nanotechnology* **2014**, *14*, 7097-7103, https://doi.org/10.1166/jnn.2014.8952.

89. Klinkova, A.; De Luna, P.; Dinh, C.T.; Voznyy, O.; Larin, E.M.; Kumacheva, E.; Sargent, E.H. Rational Design of Efficient Palladium Catalysts for Electroreduction of Carbon Dioxide to Formate. *ACS Catalysis* **2016**, *6*, 8115-8120, https://doi.org/10.1021/acscatal.6b01719.

90. Zheng, W.R.; Man, H.W.; Ye, L.; Tsang, S.C.E. Electroreduction of Carbon Dioxide to Formic Acid and Methanol over a Palladium/Polyaniline Catalyst in Acidic Solution: A Study of the Palladium Size Effect. *Energy Technology* **2017**, *5*, 937-944, https://doi.org/10.1002/ente.201600659.

91. Liu, X.; Zhu, L.S.; Wang, H.; He, G.Y.; Bian, Z.Y. Catalysis performance comparison for electrochemical reduction of CO_2 on Pd-Cu/graphene catalyst. *RSC Advances* **2016**, *6*, 38380-38387, https://doi.org/10.1039/c6ra03160a.

92. Alves, D.C.B.; Silva, R.; Voiry, D.; Asefa, T.; Chhowalla, M. Copper nanoparticles stabilized by reduced graphene oxide for CO_2 reduction reaction. *Materials for Renewable and Sustainable Energy* **2015**, *4*, https://doi.org/10.1007/s40243-015-0042-0.

93. Hossain, M.N.; Wen, J.; Chen, A. Unique copper and reduced graphene oxide nanocomposite toward the efficient electrochemical reduction of carbon dioxide. *Scientific Reports* **2017**, *7*, 3184, https://doi.org/10.1038/s41598-017-03601-3.

94. Li, F.; Xue, M.; Li, J.; Ma, X.; Chen, L.; Zhang, X.; MacFarlane, D.R.; Zhang, J. Unlocking the Electrocatalytic Activity of Antimony for CO_2 Reduction by Two-Dimensional Engineering of the Bulk Material. *Angewandte Chemie International Edition* **2017**, *56*, 14718-14722, https://doi.org/10.1002/anie.201710038.

95. Rogers, C.; Perkins, W.S.; Veber, G.; Williams, T.E.; Cloke, R.R.; Fischer, F.R. Synergistic Enhancement of Electrocatalytic CO_2 Reduction with Gold Nanoparticles Embedded in Functional Graphene Nanoribbon Composite Electrodes. *Journal of the American Chemical Society* **2017**, *139*, 4052-4061, https://doi.org/10.1021/jacs.6b12217.

96. Saquib, M.; Halder, A. Reduced graphene oxide supported gold nanoparticles for electrocatalytic reduction of carbon dioxide. *Journal of Nanoparticle Research* **2018**, *20*, https://doi.org/10.1007/s11051-018-4146-1.

97. Huang, P.; Cheng, M.; Zhang, H.; Zuo, M.; Xiao, C.; Xie, Y. Single Mo atom realized enhanced CO_2 electro-reduction into formate on N-doped graphene. *Nano Energy* **2019**, *61*, 428-434, https://doi.org/10.1016/j.nanoen.2019.05.003.

98. He, G.Y.; Tang, H.Y.; Wang, H.; Bian, Z.Y. Highly Selective and Active Pd-In/three-dimensional Graphene with Special Structure for Electroreduction CO₂ to Formate. *Electroanalysis* **2018**, *30*, 84-93, https://doi.org/10.1002/elan.201700525.

99. Song, Y.; Peng, R.; Hensley, D.K.; Bonnesen, P.V.; Liang, L.B.; Wu, Z.L.; Meyer, H.M.; Chi, M.F.; Ma, C.; Sumpter, B.G.; Rondinone, A.J. High-Selectivity Electrochemical Conversion of CO₂ to Ethanol using a Copper Nanoparticle/N-Doped Graphene Electrode. *ChemistrySelect* **2016**, *1*, 6055-6061, https://doi.org/10.1002/slct.201601169.

100. Li, Q.; Zhu, W.L.; Fu, J.J.; Zhang, H.Y.; Wu, G.; Sun, S.H. Controlled assembly of Cu nanoparticles on pyridinic-N rich graphene for electrochemical reduction of CO₂ to ethylene. *Nano Energy* **2016**, *24*, 1-9, https://doi.org/10.1016/j.nanoen.2016.03.024.

101. Sekar, P.; Calvillo, L.; Tubaro, C.; Baron, M.; Pokle, A.; Carraro, F.; Martucci, A.; Agnoli, S. Cobalt Spinel Nanocubes on N-Doped Graphene: A Synergistic Hybrid Electrocatalyst for the Highly Selective Reduction of Carbon Dioxide to Formic Acid. *ACS Catalysis* **2017**, *7*, 7695-7703, https://doi.org/10.1021/acscatal.7b02166.

102. Wang, J.; Huang, X.; Xi, S.; Lee, J.-M.; Wang, C.; Du, Y.; Wang, X. Linkage Effect in the Heterogenization of Cobalt Complexes by Doped Graphene for Electrocatalytic CO₂ Reduction. *Angewandte Chemie-International Edition* **2019**, *58*, 13532-13539, https://doi.org/10.1002/anie.201906475.

103. Su, P.; Iwase, K.; Nakanishi, S.; Hashimoto, K.; Kamiya, K. Nickel-Nitrogen-Modified Graphene: An Efficient Electrocatalyst for the Reduction of Carbon Dioxide to Carbon Monoxide. *Small* **2016**, *12*, 6083-6089, https://doi.org/10.1002/smll.201602158.

104. Zhang, S.; Kang, P.; Ubnoske, S.; Brennaman, M.K.; Song, N.; House, R.L.; Glass, J.T.; Meyer, T.J. Polyethylenimine-enhanced electrocatalytic reduction of CO₂ to formate at nitrogen-doped carbon nanomaterials. *Journal of the American Chemical Society* **2014**, *136*, 7845-7848, https://doi.org/10.1021/ja5031529.

105. Sharma, P.P.; Wu, J.; Yadav, R.M.; Liu, M.; Wright, C.J.; Tiwary, C.S.; Yakobson, B.I.; Lou, J.; Ajayan, P.M.; Zhou, X.D. Nitrogen-Doped Carbon Nanotube Arrays for High-Efficiency Electrochemical Reduction of CO₂: On the Understanding of Defects, Defect Density, and Selectivity. *Angewandte Chemie International Edition* **2015**, *54*, 13701-13705, https://doi.org/10.1002/anie.201506062.

106. Xu, J.; Kan, Y.; Huang, R.; Zhang, B.; Wang, B.; Wu, K.H.; Lin, Y.; Sun, X.; Li, Q.; Centi, G., et al. Revealing the Origin of Activity in Nitrogen-Doped Nanocarbons towards Electrocatalytic Reduction of Carbon Dioxide. *ChemSusChem* **2016**, *9*, 1085-1089, https://doi.org/10.1002/cssc.201600202.

107. Sun, X.; Kang, X.; Zhu, Q.; Ma, J.; Yang, G.; Liu, Z.; Han, B. Very highly efficient reduction of CO₂ to CH₄ using metal-free N-doped carbon electrodes. *Chemical Science* **2016**, *7*, 2883-2887, https://doi.org/10.1039/c5sc04158a.

108. Soliman, A.; Haikal, R.; Hassan,Y.; Alkordi, M. *Chemical Communications,* **2016**, *52*, 12032-12035, https://doi.org/10.1039/c6cc06773e.

109. Sreekanth, N.; Nazrulla, M.A.; Vineesh, T.V.; Sailaja, K.; Phani, K.L. Metal-free boron-doped graphene for selective electroreduction of carbon dioxide to formic acid/formate. *Chemical Communications,* **2015**, *51*, 16061-16064, https://doi.org/10.1039/c5cc06051f.

8. ACKNOWLEDGEMENTS